DIS2016, DESY, Hamburg

April 12th, 2016

Measurement of photon production cross sections with the ATLAS detector

J. Terrón (Universidad Autónoma de Madrid)

On behalf of the ATLAS Collaboration

- **Outline**
  - → Physics with photons
  - → Photons with the ATLAS detector
  - → Inclusive photon production at 8 TeV
  - → Inclusive photon production at 13 TeV
  - → Summary

Photon production in pp collisions at LHC

- **Photon production in pp collisions allows**

  $\rightarrow$ tests of perturbative QCD

  $\rightarrow$ to extract information on the proton PDFs

- **Possibilities to study inclusive production of photons or in association with jets**

- **Prompt photons represent a cleaner probe of the hard interaction than jet production**

- **Of special interest as the 2nd largest source of background to $H \rightarrow \gamma\gamma$**

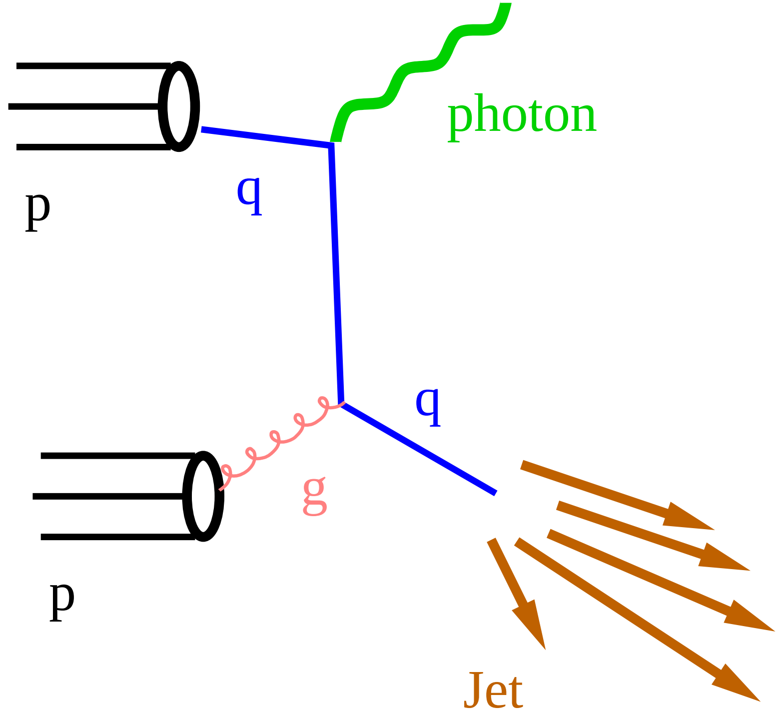

Other sources of photons

- **Quarks and gluons are sources of photons**

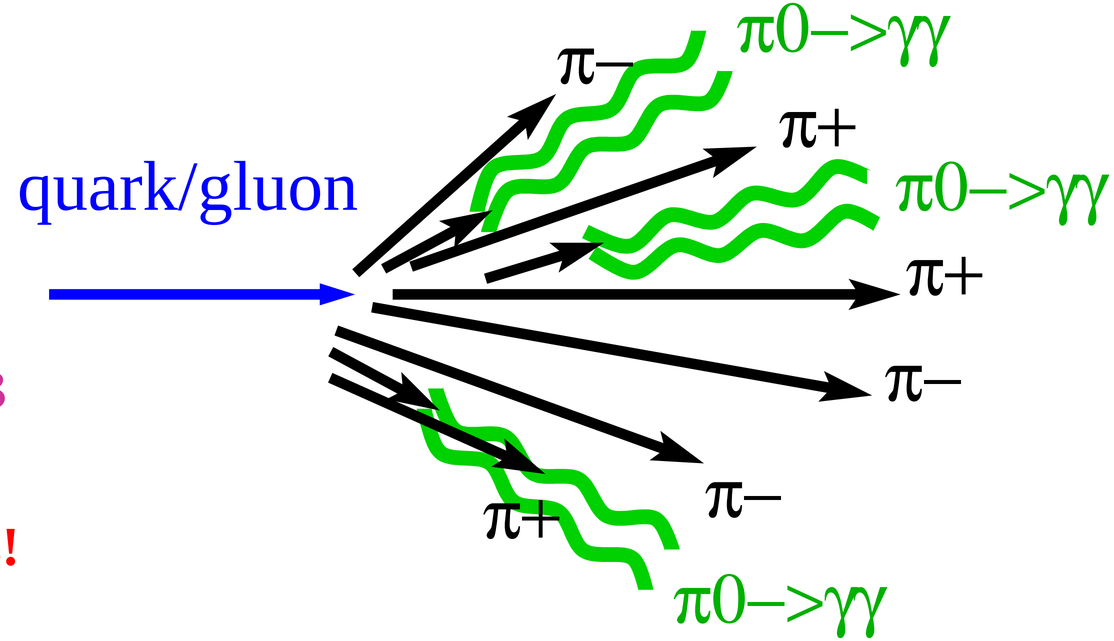

→ Quarks and gluons hadronize mostly into pions and, by isospin symmetry, 1/3 are π^0's, which decay into two photons

⇒ γ's are produced copiously inside jets!

→ Quarks have electric charge and radiate photons

⇒ fragmentation function $D^{\gamma}_{q/g}(z, \mu_f)$

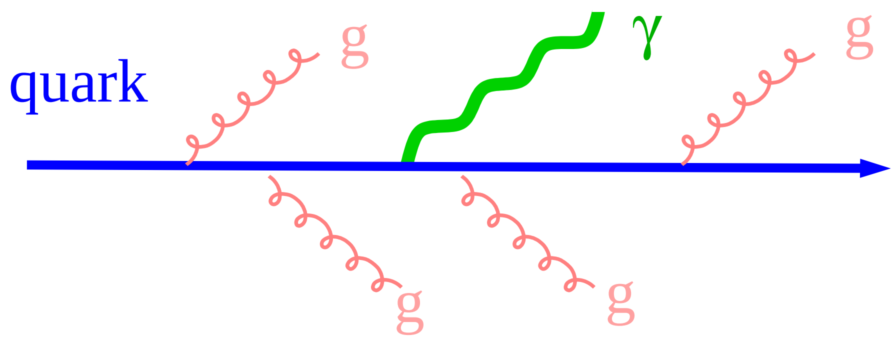

⇒ Distinct feature: these photons are inside jets, i.e. not isolated!

Photon isolation

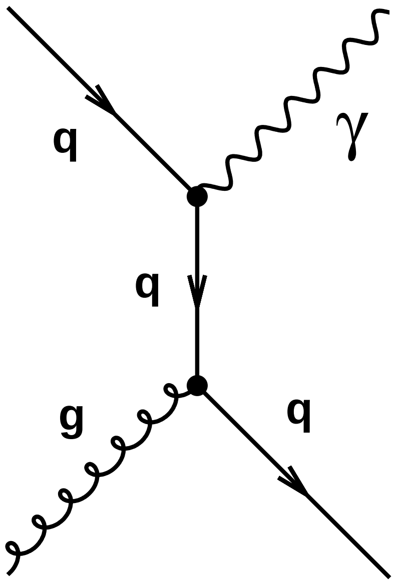

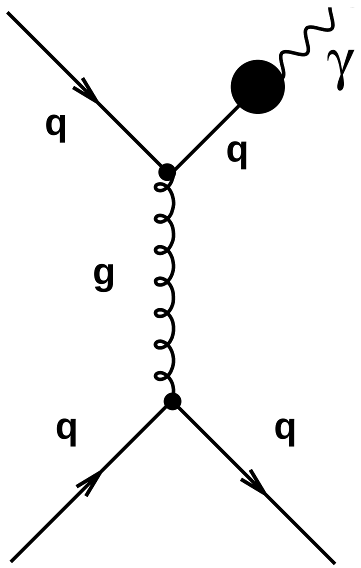

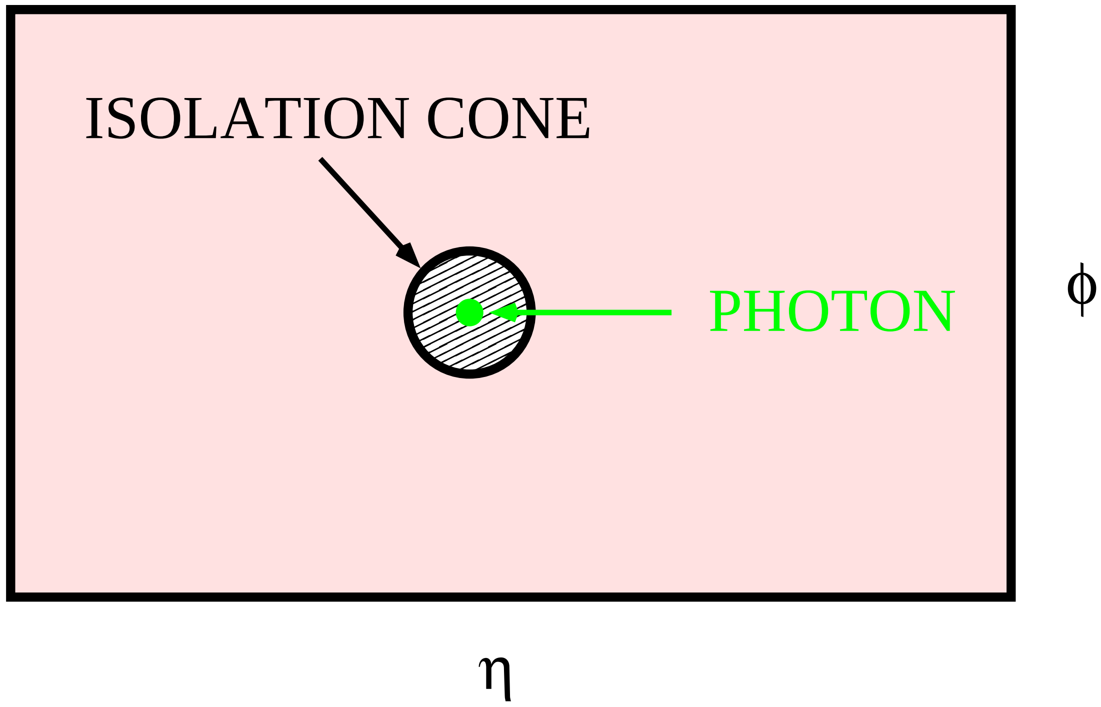

- It is essential to require the photon to be isolated. It is achieved by requiring $E_T^{iso} \equiv \sum_i E_T^i < E_T^{\max}$ with the sum over the particles (except the photon!) inside a cone of radius $R = 0.4$ centered on the photon in the $\eta - \phi$ plane

  $\rightarrow$ **For the analyses presented here:** $E_T^{\max} = 4.2 \cdot 10^{-3} \cdot E_T^{\gamma} + 4.8$ **GeV**

- The isolation requirement suppresses the contribution of photons inside jets: π^0 (as well as other neutral mesons) decays and the fragmentation contribution

NLO QCD calculations for inclusive photon production

$$\sigma_{pp\to\gamma+X} = \sum_{i,j,a} \int_0^1 dx_1\, f_{i/p}(x_1,\mu_F^2) \int_0^1 dx_2\, f_{j/p}(x_2,\mu_F^2)\ \hat{\sigma}_{ij\to\gamma a} +$$

$$\sum_{i,j,a,b} \int_{z_{min}}^1 dz\, D_a^\gamma(z,\mu_f^2) \int_0^1 dx_1\, f_{i/p}(x_1,\mu_F^2) \int_0^1 dx_2\, f_{j/p}(x_2,\mu_F^2)\ \hat{\sigma}_{ij\to ab}$$

- The calculations include NLO corrections for both direct-photon and fragmentation contributions; beware the components are not distinguishable beyond LO
- Isolation at "parton level": E_T^{iso} calculated with the (few) final-state partons
- Using the JetPhox program (S. Catani, M. Fontannaz, J. Ph. Guillet and E. Pilon) with

  $\rightarrow \mu_R = \mu_F = \mu_f = E_T^\gamma$ (nominal) $\rightarrow$ proton PDF set: CT10

  $\rightarrow$ fragmentation function: BFG set II

$\rightarrow$ Corrections for hadronisation and underlying event needed

- Theoretical uncertainties:

$\rightarrow$ terms beyond NLO; varying μ_R, μ_F, μ_f by factors 2 and $1/2$ (singly or simultaneously)

$\rightarrow$ PDF-induced uncertainties; estimated using set of PDF eigenvectors

$\rightarrow$ uncertainty on α_s; estimated using PDFs in which different values of α_s are assumed

$\rightarrow$ uncertainty on non-perturbative correction; estimated with different MCs

Photons with the ATLAS detector

Photon reconstruction in the ATLAS LAr Calorimeter

- **Layout of the ATLAS electromagnetic calorimeter (Lead-liquid Argon)**

$\rightarrow$ **barrel section, $|\eta| < 1.475$**
$\rightarrow$ **two end-cap sections, $1.375 < |\eta| < 3.2$**
$\rightarrow$ **three longitudinal layers**

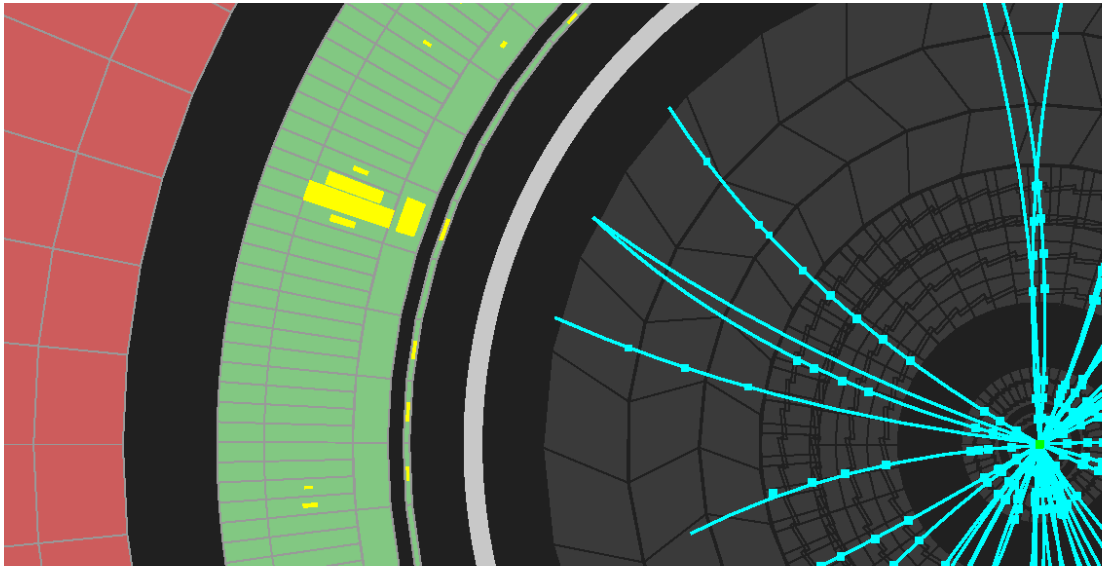

— First layer: high granularity in η direction, width 0.003-0.006 (except for $1.4 < |\eta| < 1.5$ and $|\eta| > 2.4$)

— Second layer: collects most of the energy, granularity 0.025×0.025 in $\eta \times \phi$

— Third layer: used to correct for leakage

- **Cluster of EM cells without matching track:**

$\rightarrow$ **"unconverted" photon candidate**

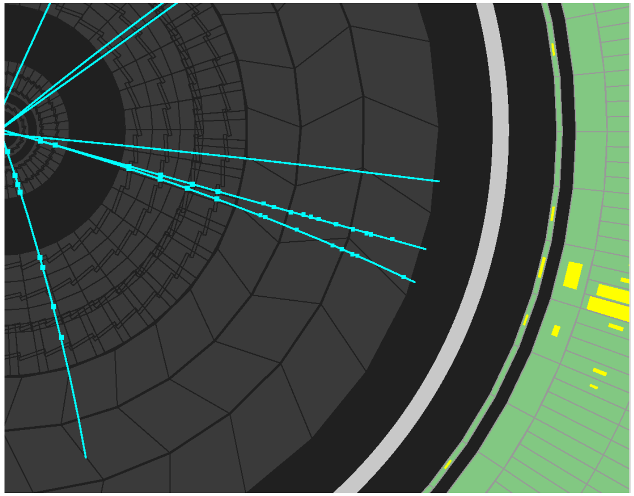

- **Cluster of EM cells matched to pairs of tracks (from reconstructed conversion vertices in the inner detector) or matched to a single track consistent with originating from a photon conversion**

$\rightarrow$ **"converted" photon candidate**

Photon identification in the ATLAS LAr Calorimeter

- **To discriminate signal vs background:** shape variables from the lateral and longitudinal energy profiles of the shower in the calorimeters; "loose" and "tight" identification criteria.

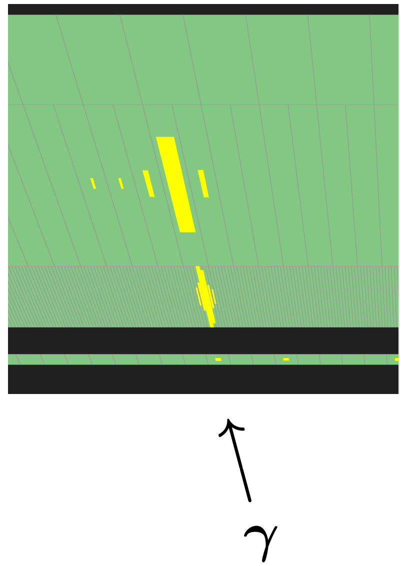

- **"Loose" identification criteria:**

$\rightarrow$ leakage $R_{had} = E_T^{had}/E_T$ (1st layer hadronic calorimeter)

$\rightarrow$ $R_\eta = E^{S2}_{3\times7}/E^{S2}_{7\times7}$; $S2$=second layer of EM calorimeter

$\rightarrow$ RMS width of the shower in η direction in $S2$

- **"Tight" identification criteria:**

$\rightarrow$ the requirements applied in "Loose" are tightened

$\rightarrow$ $R_\phi = E^{S2}_{3\times3}/E^{S2}_{3\times7}$

and shower shapes in the first layer (to discriminate single-photon showers from overlapping nearby showers, such as $\pi^0 \rightarrow \gamma\gamma$)

$\rightarrow$ e.g. asymmetry between the 1st and 2nd maxima in the energy profile along η ($S1$)

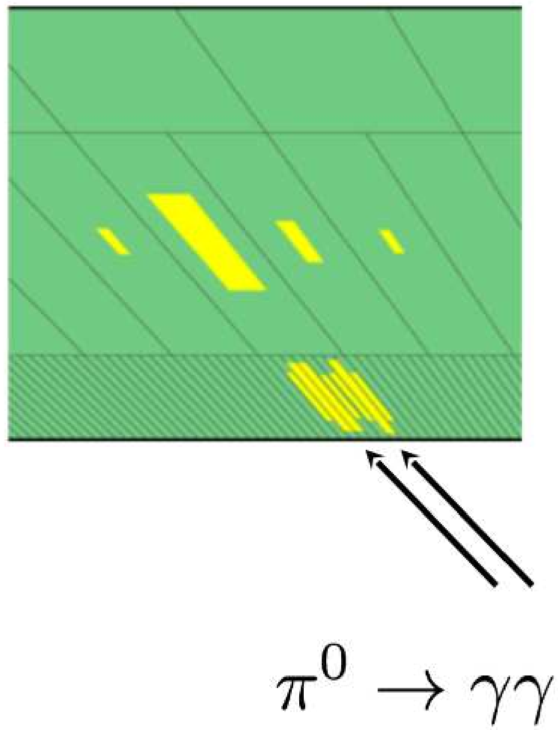

Photon identification efficiency

ATLAS Coll., ATLAS-CONF-2012-123

CONVERTED PHOTONS

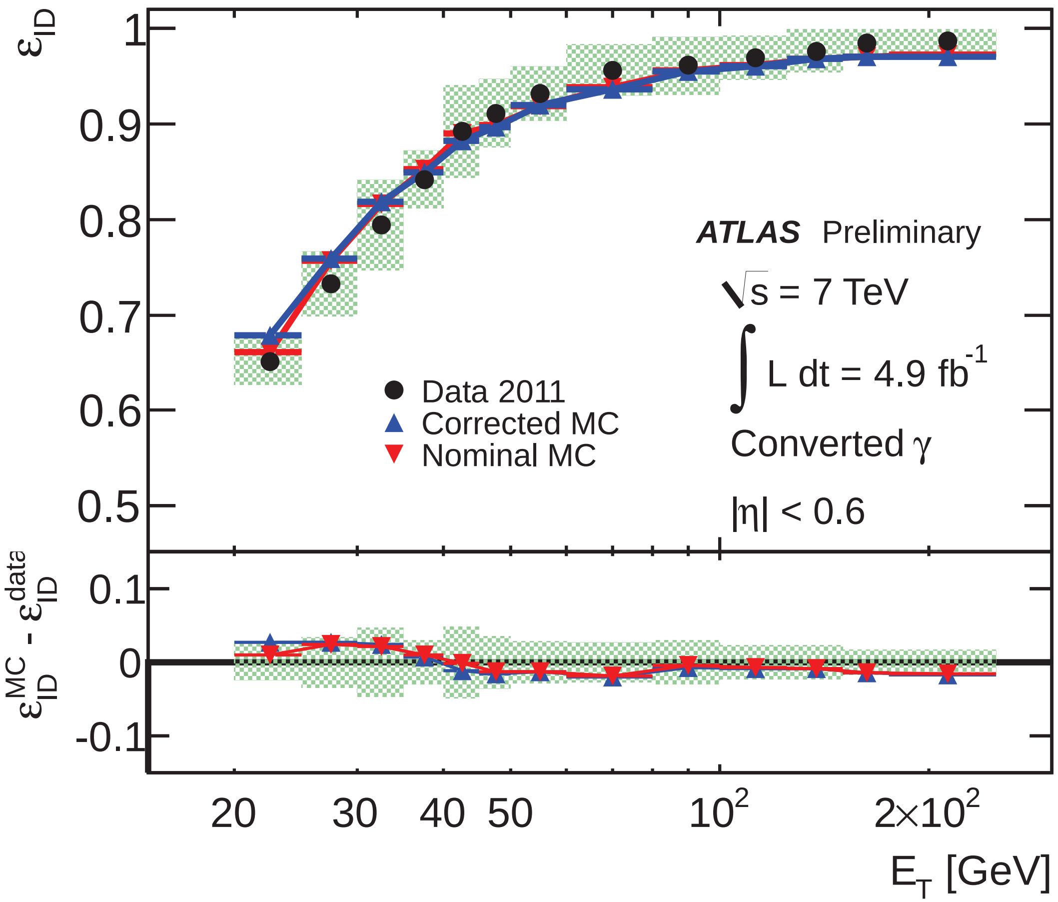

UNCONVERTED PHOTONS

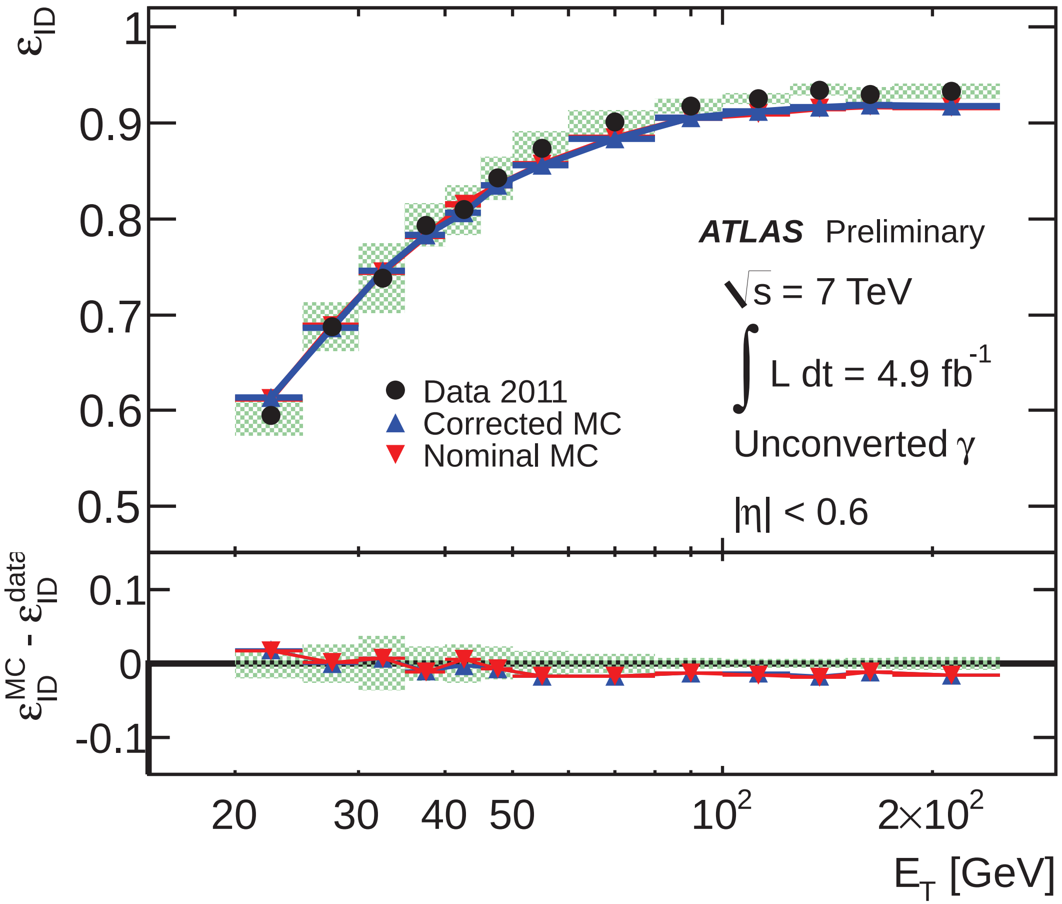

- **Data-driven measurements of photon identification efficiency for converted and unconverted photons (radiative Z decays, extrapolation from $e^{\pm}$ and matrix method) compared to estimations based on Monte Carlo simulations**

Photon isolation in ATLAS

- $E_T^{iso}(R = 0.4)$ computed using clusters of calorimeter cells (EM and HAD) in a cone $R = 0.4$, excluding the contribution from the photon
- Subtraction of the leakage of the photon energy outside that region (few %)
- The underlying event and pileup (overlapping pp interactions in the same/neighbouring bunch crossings) contribute to E_T^{iso}!
Subtracted on event-by-event basis using the jet-area method of M. Cacciari et al
- After isolation requirement, residual background still expected

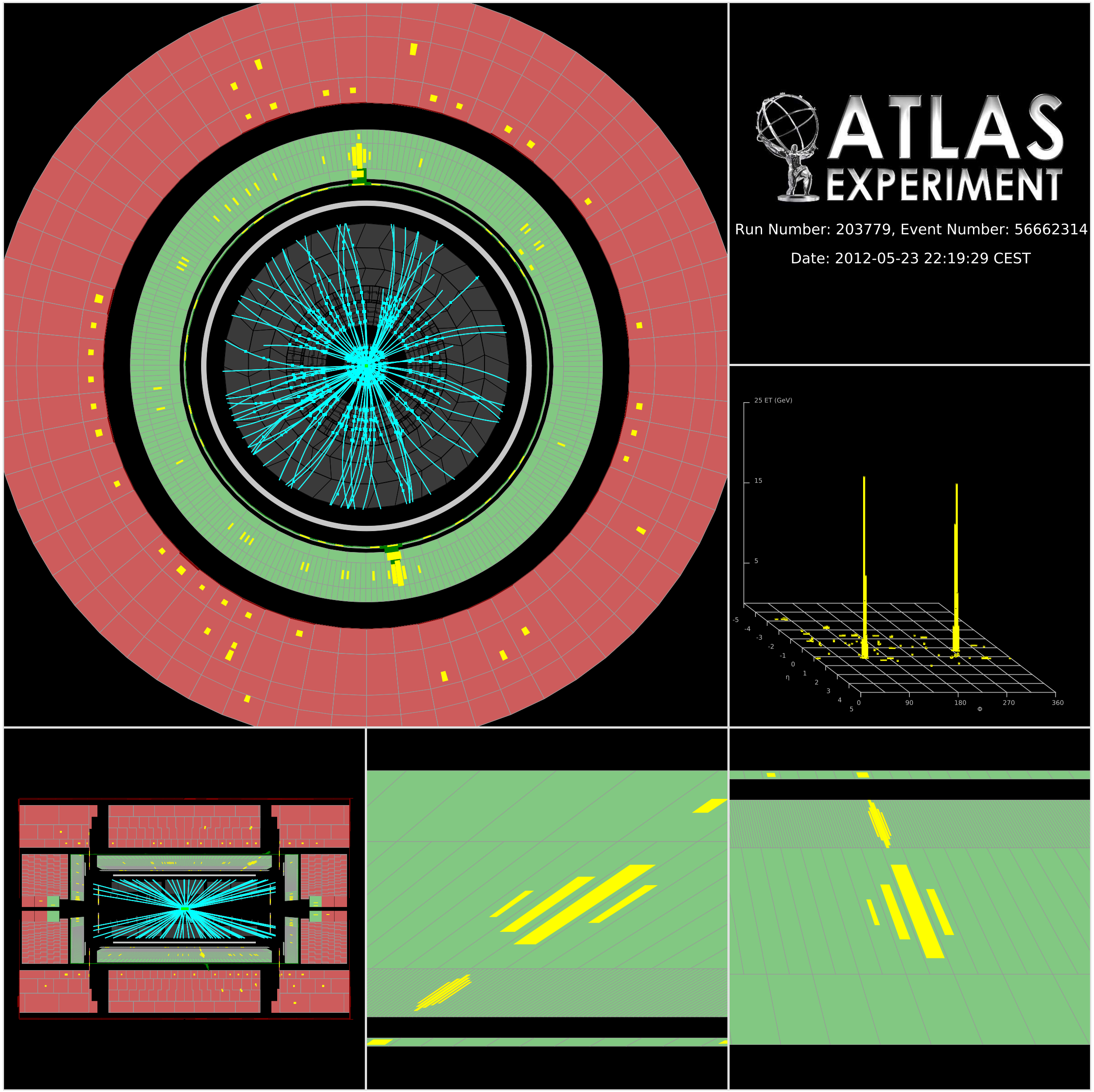

Background subtraction

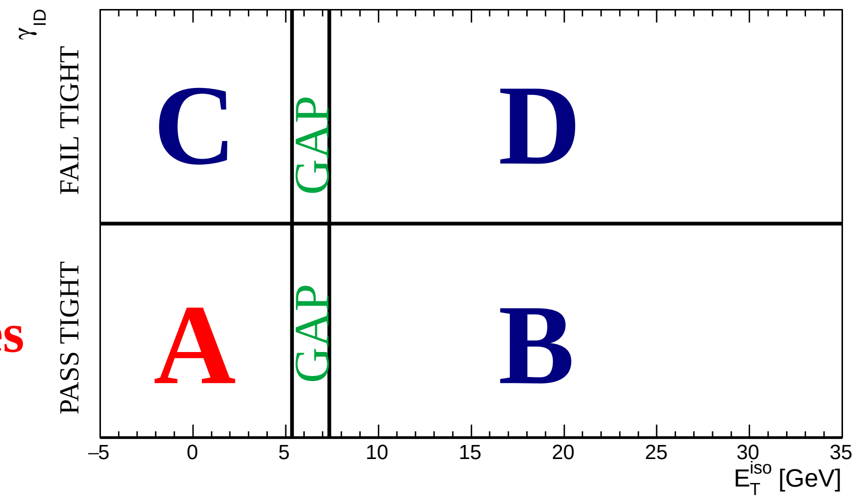

- **Residual background still expected even after the tight identification and isolation requirements**
- **A data-driven method necessary to avoid relying on detailed simulations of the background processes**
- **The two-dimensional sideband method:**

→ photon identification γ_{ID} vs E_T^{iso} plane

- **It is assumed that for background events there is no correlation between γ_{ID} and E_T^{iso}**

$$\frac{N_A^{bkg}}{N_B^{bkg}} = \frac{N_C^{bkg}}{N_D^{bkg}} \qquad \Rightarrow R_{bkg} \equiv \frac{N_A^{bkg} \cdot N_D^{bkg}}{N_B^{bkg} \cdot N_C^{bkg}} = 1$$

and the effects of the small signal contaminations can be accounted for by using

$$\frac{N_A - N_A^{sig}}{N_B - \epsilon_B N_A^{sig}} = \frac{N_C - \epsilon_C N_A^{sig}}{N_D - \epsilon_D N_A^{sig}}$$

to extract the signal yield N_A^{sig}

the leakage fractions ($\epsilon_K \equiv N_K^{sig}/N_A^{sig}, K = B, C, D$) are estimated using MC samples of signal ⇒ purity rises from 60% ($E_T^\gamma \sim 25$ GeV) to 100% ($E_T^\gamma \sim 300$ GeV)

Inclusive photon production at 8 TeV

Inclusive isolated-photon production in pp collisions at $\sqrt{s} = 8$ TeV

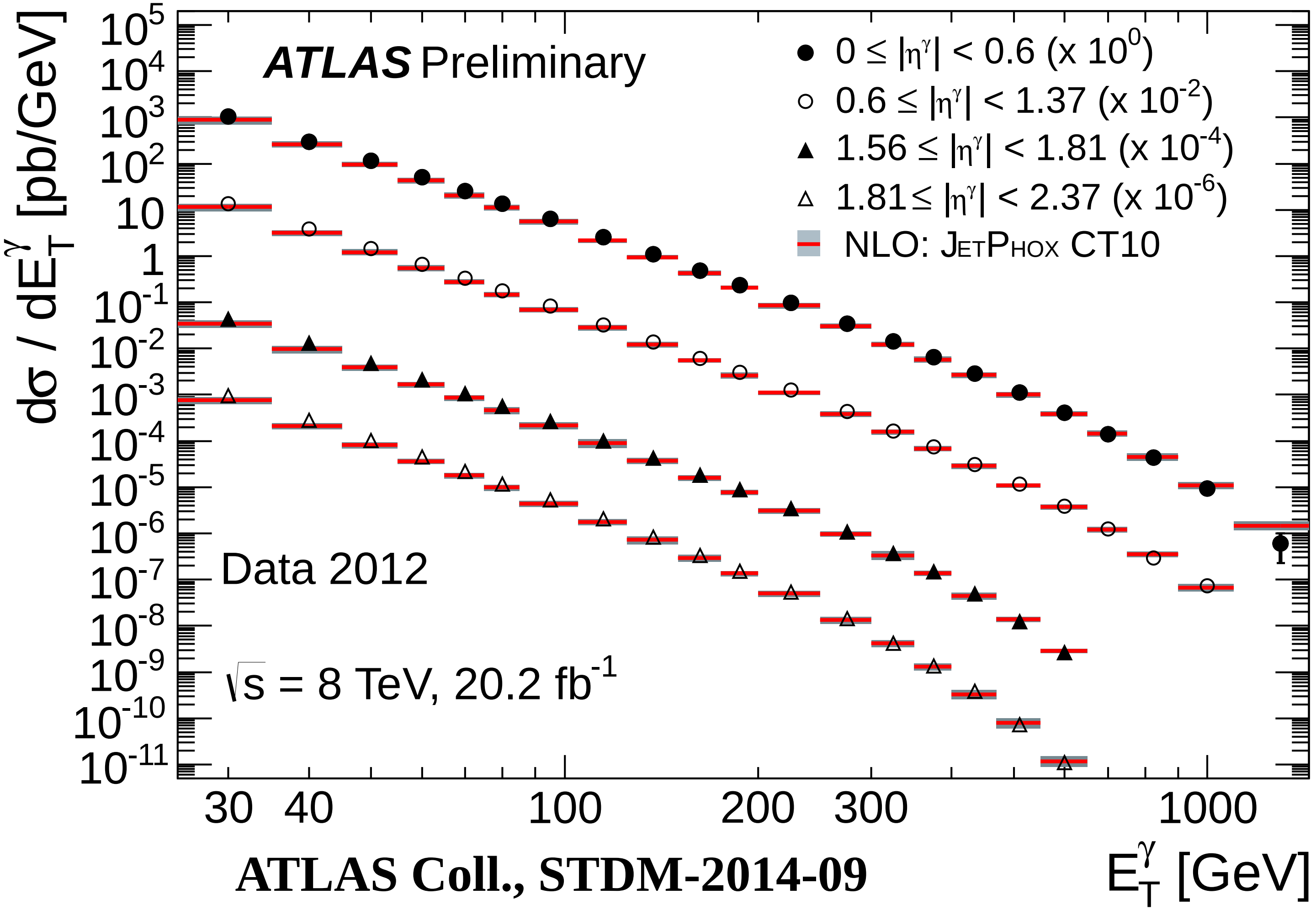

ATLAS Coll., STDM-2014-09

- Measurement of $d\sigma/dE_T^{\gamma}$ for $25 < E_T^{\gamma} < 1500$ GeV and different ranges in η^{γ} using $\mathcal{L} = 20.2$ fb^{-1} of pp collision data at $\sqrt{s} = 8$ TeV
- The measurement covers ten orders of magnitude in cross section
- First measurement of photon production with $E_T^{\gamma} > 1$ TeV

- Significant improvement in experimental uncertainties over the previous measurements
- Good description (in log scale) of the data by NLO QCD calculations using JetPhox

Major experimental uncertainties

ATLAS Coll., STDM-2014-09

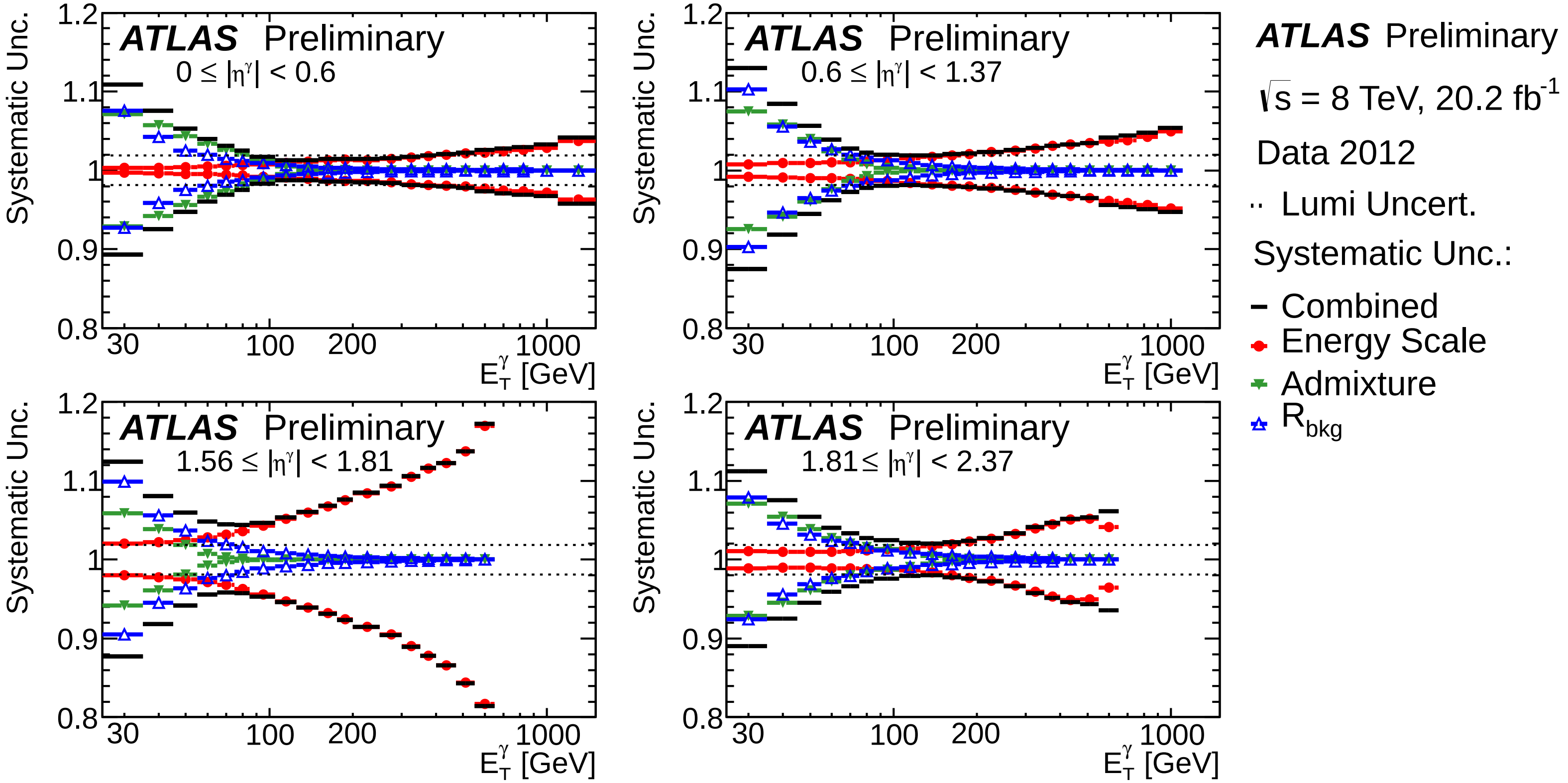

- **The uncertainty on the photon energy scale* (about 1% except in the region $1.56 < |\eta^\gamma| < 1.81$) is dominant at high E_T^γ**

  * (ATLAS Collaboration, Eur. Phys. J. C74 (2014) 3071)
- **The uncertainty on the correlation in the background ($\pm 10\%$) dominates at low E_T^γ, but negligible at high E_T^γ**
- **The uncertainty on the admixture of direct and fragmentation photons increases at low E_T^γ**

Inclusive isolated-photon cross sections vs NLO QCD

ATLAS Coll., STDM-2014-09

Theoretical uncertainties much larger than(!) experimental uncertainties

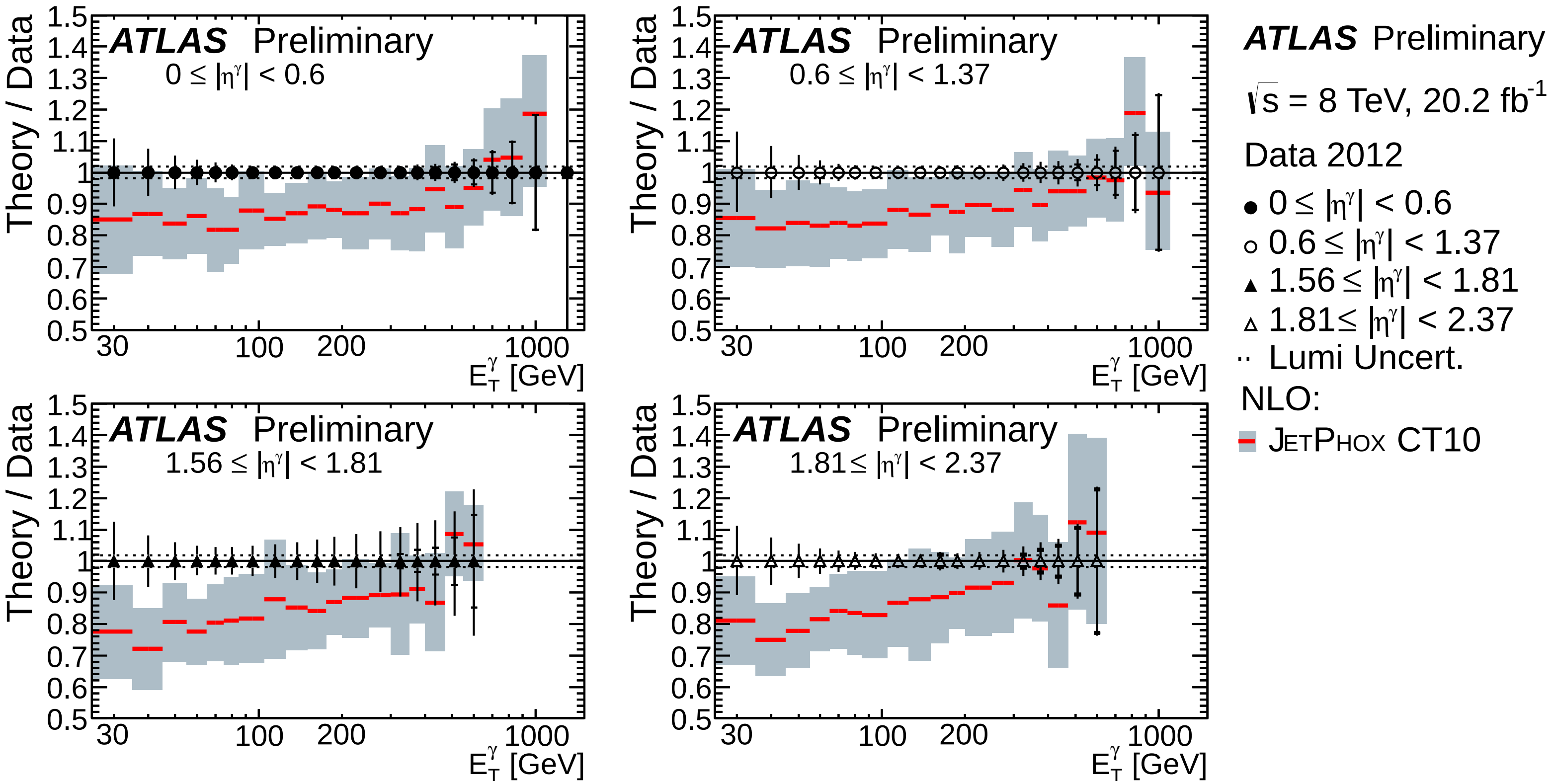

- **Comparison to NLO QCD calculation using the JetPhox program**
  - → **a similar trend is observed at low E_T^γ in all $|\eta^\gamma|$ regions, the NLO QCD predictions underestimate the data by ≈ 20%**
  - → **the theoretical uncertainty (12-20%) prevents a more precise test of the SM predictions**
- **Halving the measured uncertainties compared to previous measurements**
  - ⇒ **useful constraint on proton PDFs once included in a global fit**

Inclusive isolated-photon cross sections vs improved NLO QCD

Still theoretical uncertainties much larger than(!) experimental uncertainties

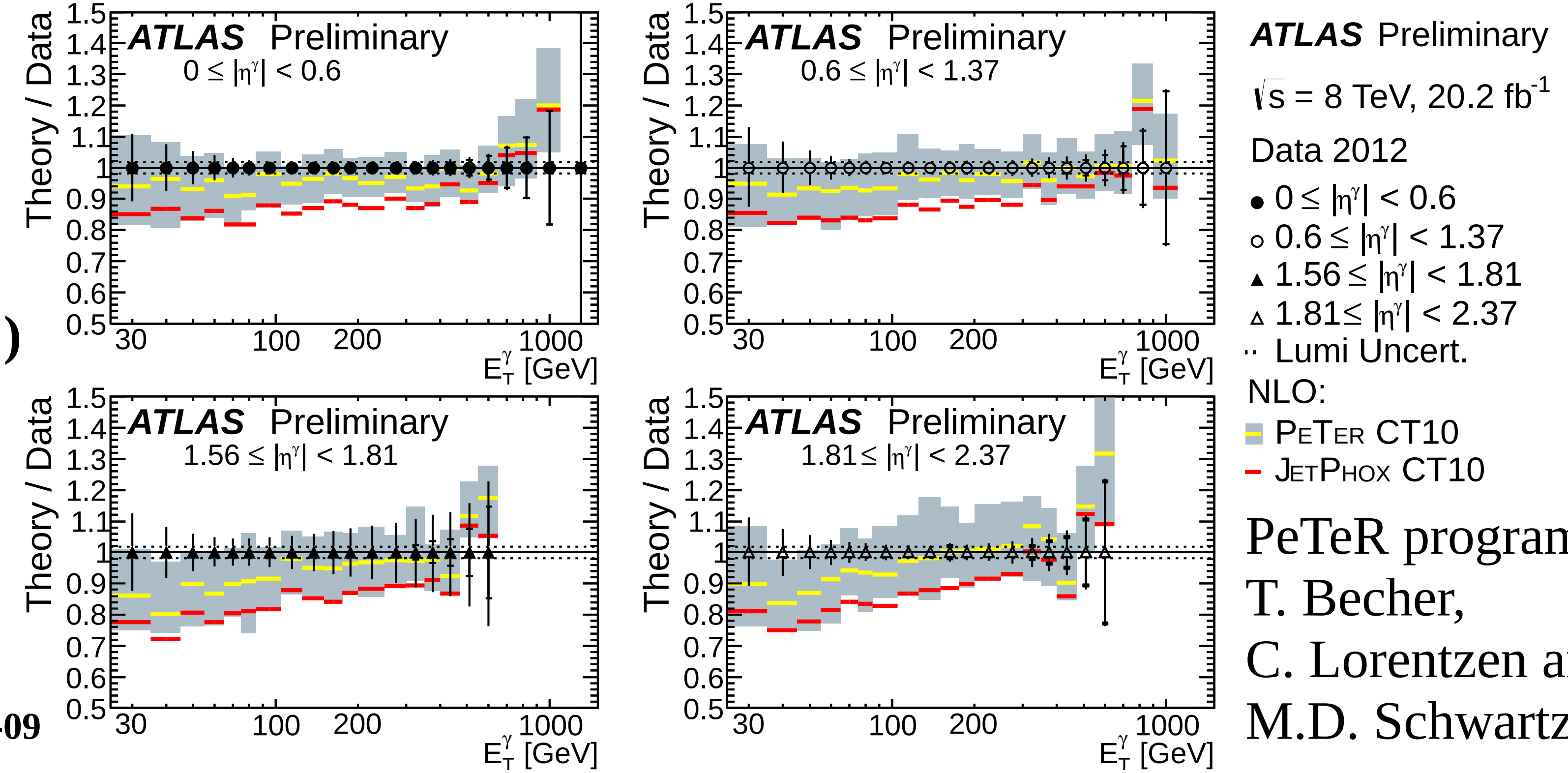

ATLAS Coll., STDM-2014-09

PeTeR program
T. Becher,
C. Lorentzen and
M.D. Schwartz

- **Comparison to improved NLO QCD calculations using the PeTeR program: resummation of QCD threshold logarithms at NNNLL and large electroweak Sudakov logarithms**
  - **→ improved description of the data: PeTeR vs JetPhox**
  - **→ reduction of the theoretical uncertainty: ∼ 20% smaller than in NLO QCD (JetPhox)**

Inclusive photon production at 13 TeV

Inclusive isolated-photon production in pp collisions at $\sqrt{s} = 13$ TeV

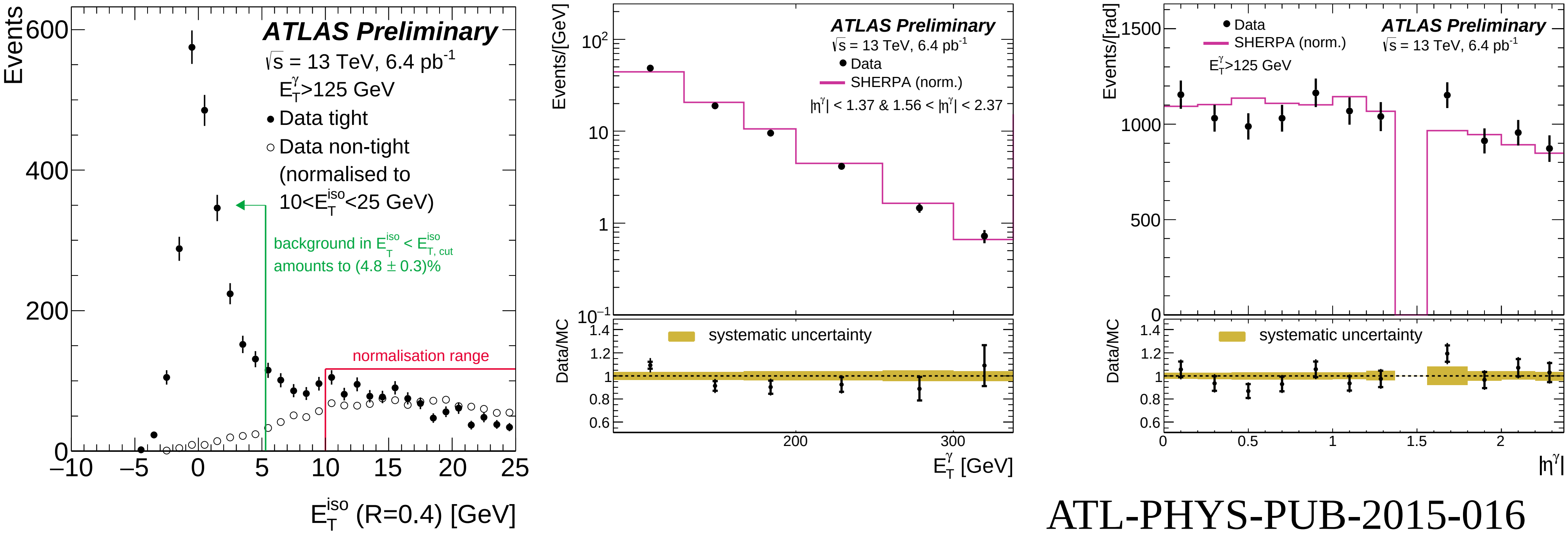

ATL-PHYS-PUB-2015-016

- **First study of inclusive isolated-photon production in pp collisions at 13 TeV using $\mathcal{L} = 6.4$ pb^{-1} and covering the ranges $125 < E_T^\gamma < 350$ GeV and $|\eta^\gamma| < 2.37$ (except for $1.37 < |\eta^\gamma| < 1.56$)**
- **Background subtraction using a data-driven technique based on the $E_T^{\rm iso}$ distribution**
- **Good description of the shape of the measured distributions in E_T^γ and $|\eta^\gamma|$ by the predictions of Sherpa 2.1 in the new regime opened by the LHC in 2015**

Summary

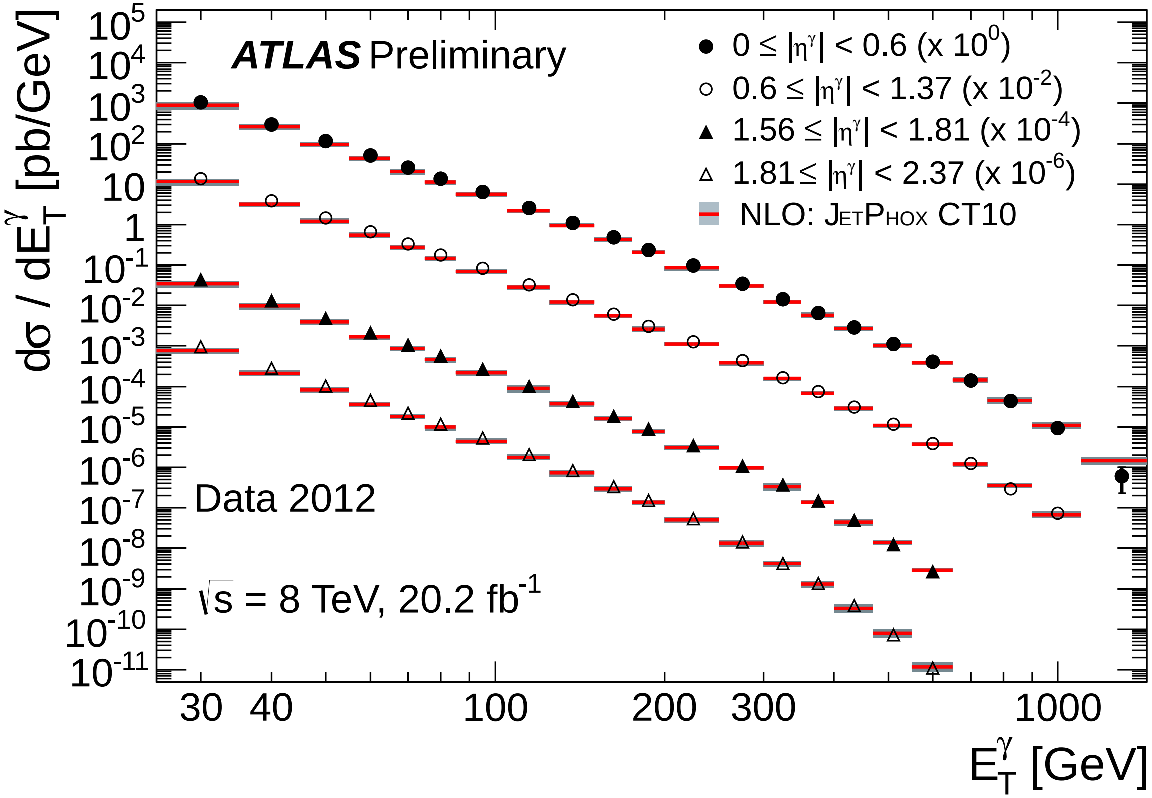

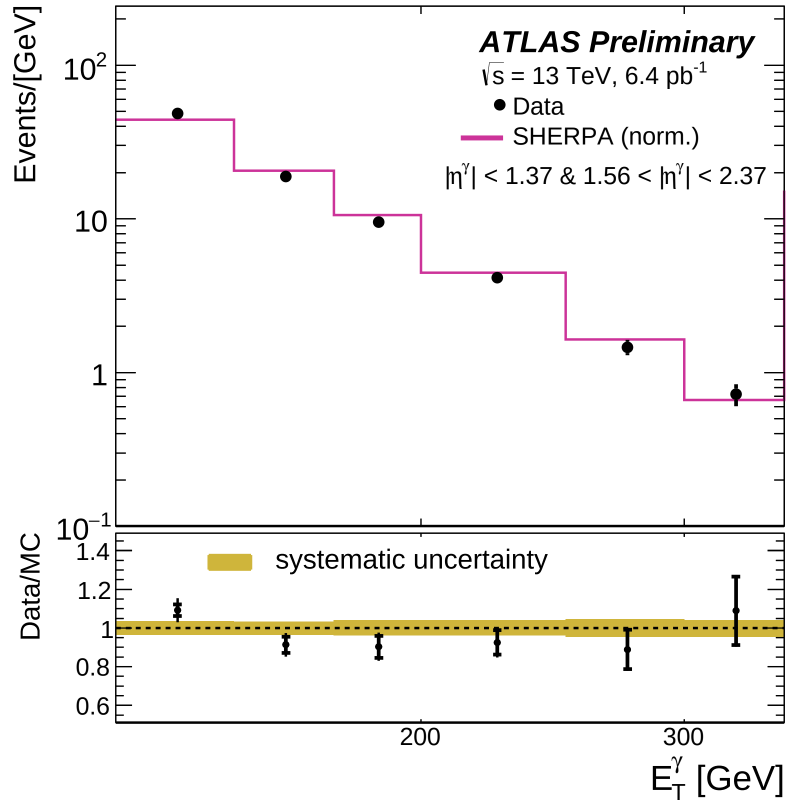

- Measurement of isolated photon production in pp collisions at $\sqrt{s} = 8$ TeV in the range $25 < E_T^\gamma < 1500$ GeV with improved experimental uncertainties

$\Rightarrow$ NLO QCD supplemented with resummation+electroweak corrections describe the data

$\Rightarrow$ theoretical $\gg$ experimental uncertainties, room for improvement with better calculations

$\Rightarrow$ experimental information to constrain further the proton parton densities

- First look at inclusive isolated photon production in pp collisions at $\sqrt{s} = 13$ TeV

Backup

Corrections for non-perturbative effects; photon isolation

- The measurements are corrected for detector effects to the "particle" level
  $\rightarrow$ to isolated photons, where E_T^{iso} is calculated using all the final-state particles and the jet-area method is also applied
  This is performed using MC simulations

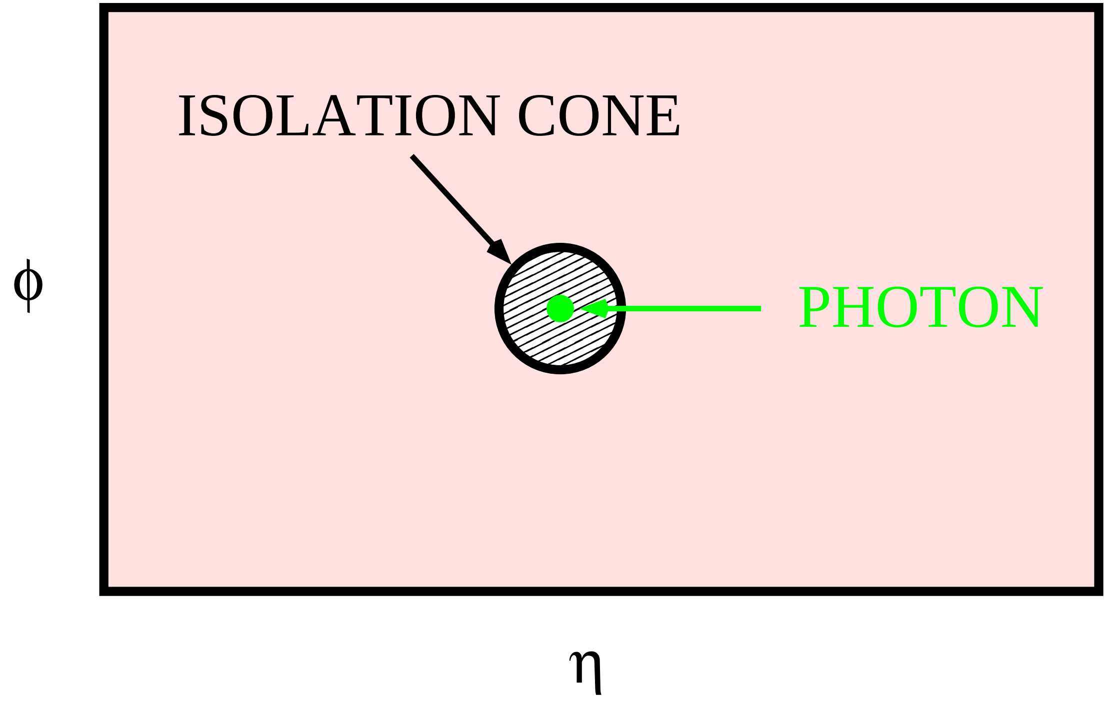

- Corrections for non-perturbative effects (hadronisation and underlying event)

$$C_{NP} = \frac{\sigma_{\gamma+\mathrm{X}}(\mathrm{MC, particle-level, UE})}{\sigma_{\gamma+\mathrm{X}}(\mathrm{MC, parton-level, no\ UE})}$$

$\rightarrow$ Less dependence on the modelling of the final state by having used the jet-area method to subtract the "extra" transverse energy contribution to E_T^{iso}

$\Rightarrow$ The resulting C_{NP} is found to be consistent with 1 for the measurements presented here

Impact of inclusive isolated photon measurements at LHC on PDFs

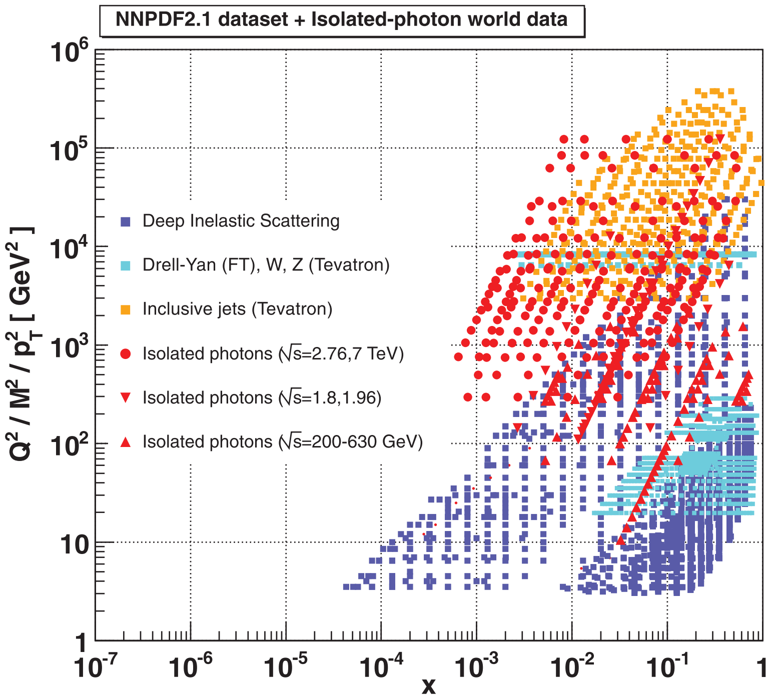

- **Analysis by D. d'Enterria and J. Rojo** (Nucl. Phys. B860 (2012) 311)
- **Study of the impact on the gluon density of existing isolated-photon measurements from a variety of experiments, from $\sqrt{s} = 200$ GeV up to 7 TeV**
  - **$\rightarrow$ those at LHC are the more constraining datasets**
  - **$\rightarrow$ reduction of gluon uncertainty up to 20%**
  - **$\rightarrow$ localised in the range $x \approx 0.002$ to 0.05**

$\Rightarrow$ improved predictions for low mass Higgs production in gluon fusion, PDF-induced uncertainty decreased by 20%

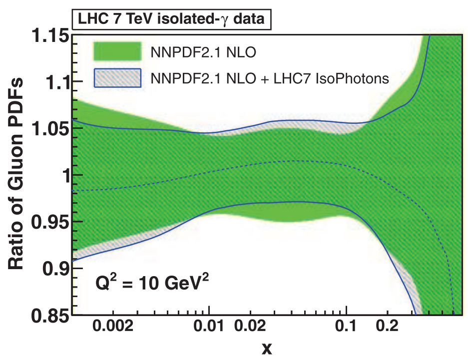

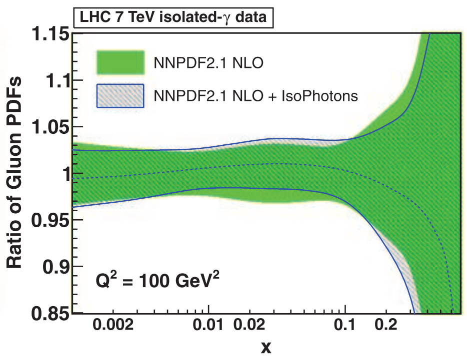

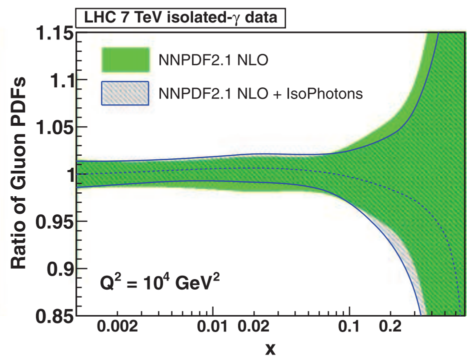

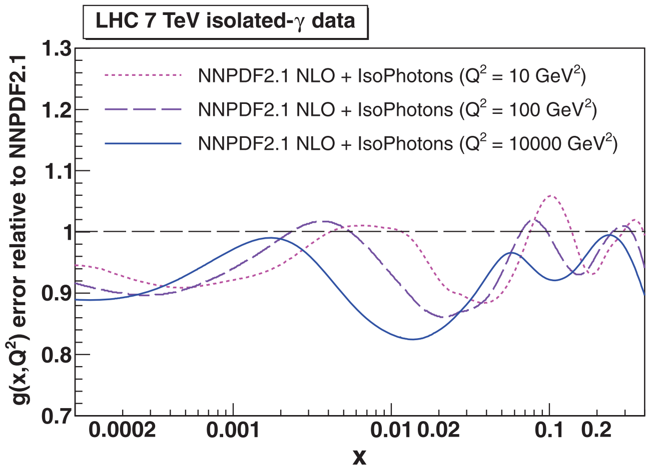

The ATLAS detector

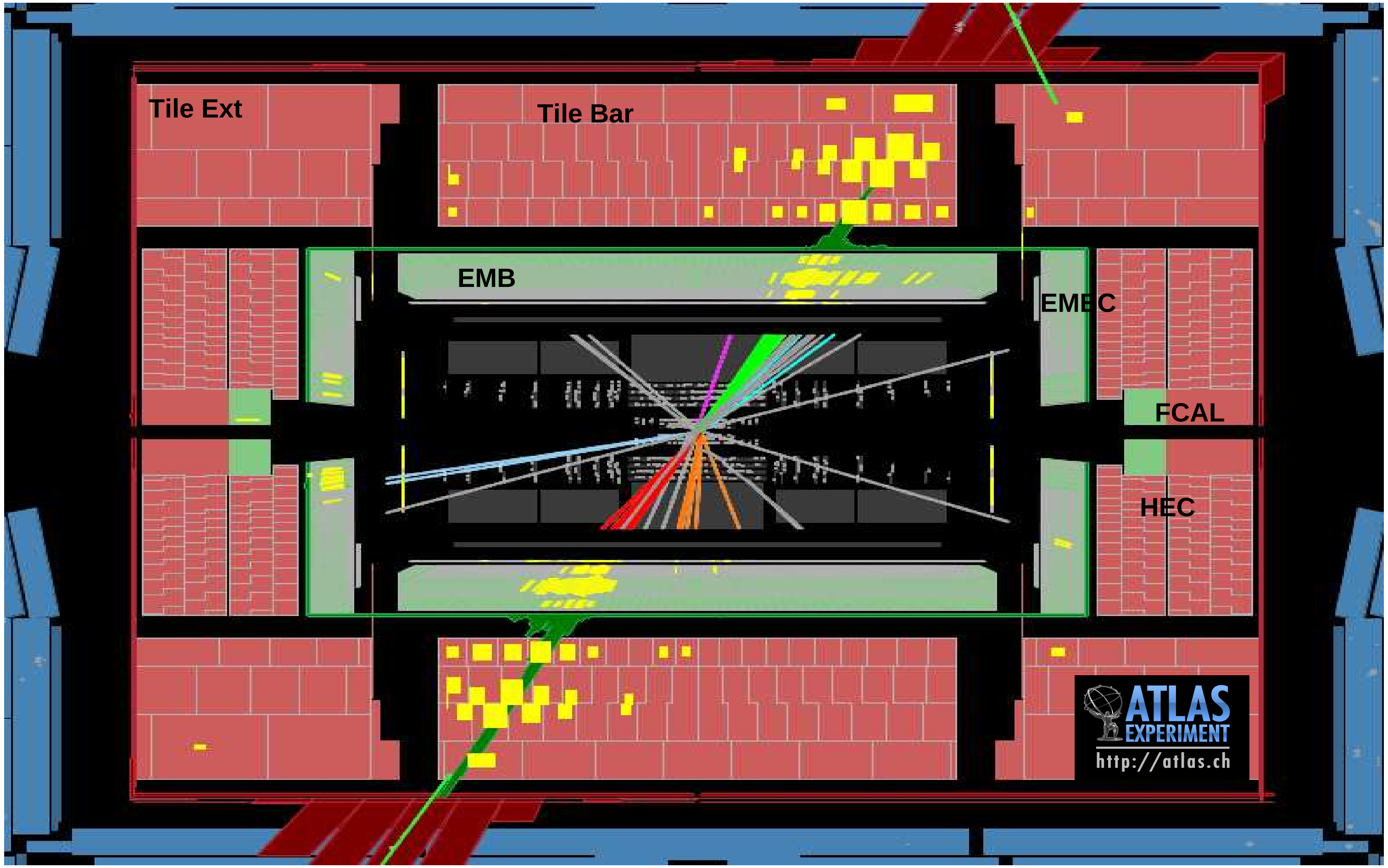

- Inner detector (ID): tracking and particle identification in $|\eta| < 2.5$
- Calorimeters: electromagnetic (LAr) $\rightarrow$ barrel $|\eta| < 1.475$, endcap $1.375 < |\eta| < 3.2$, forward $3.1 < |\eta| < 4.9$; hadronic (scintillator/steel, LAr/Cu, LAr/W) $\rightarrow$ barrel $|\eta| < 0.7$ extended barrel $0.8 < |\eta| < 1.7$, endcap $1.5 < |\eta| < 3.2$ and forward $3.1 < |\eta| < 4.9$

Electron and photon calibration in ATLAS

ATLAS Collaboration, Eur. Phys. J. C74 (2014) 3071

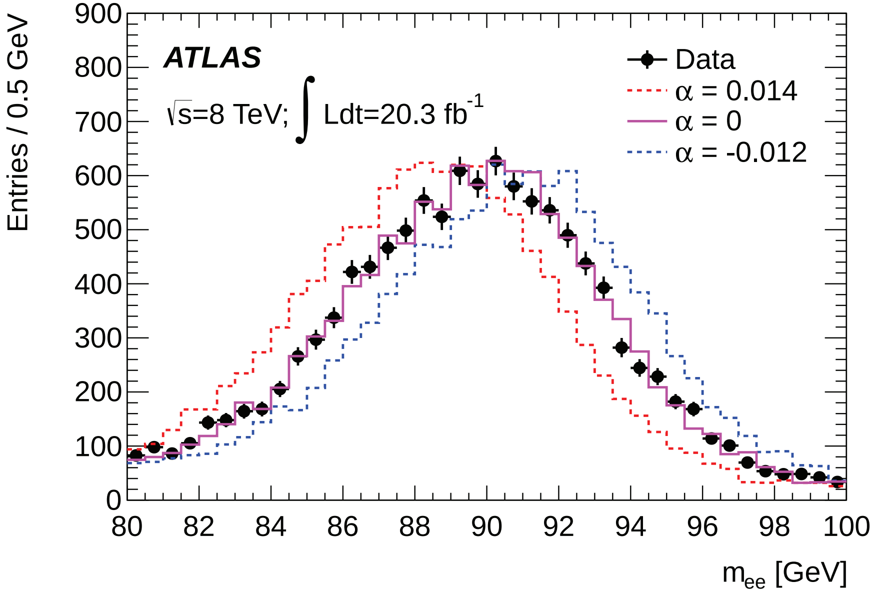

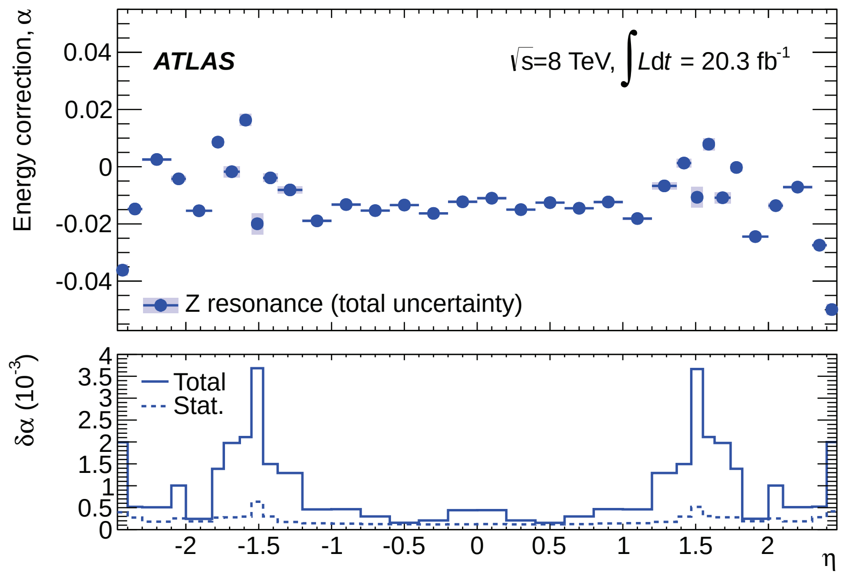

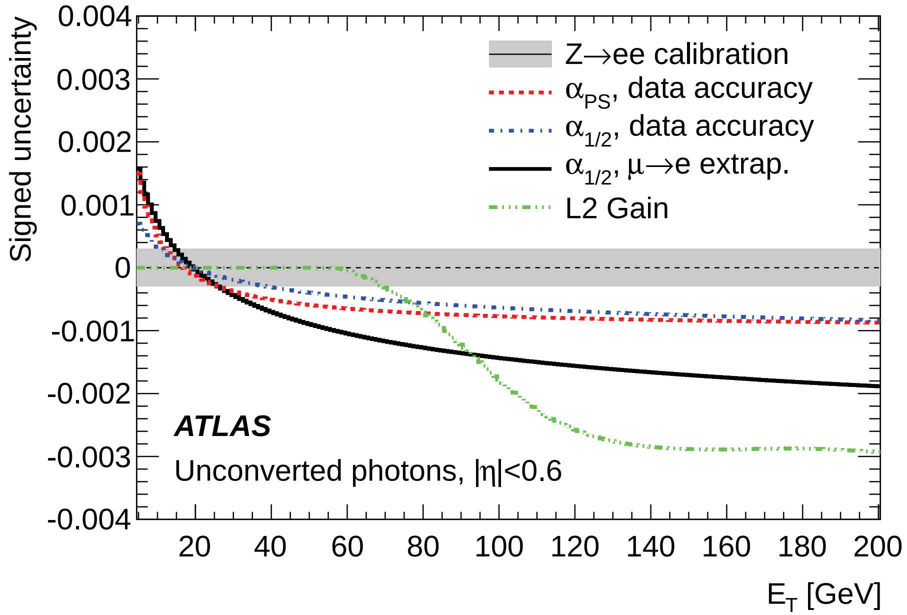

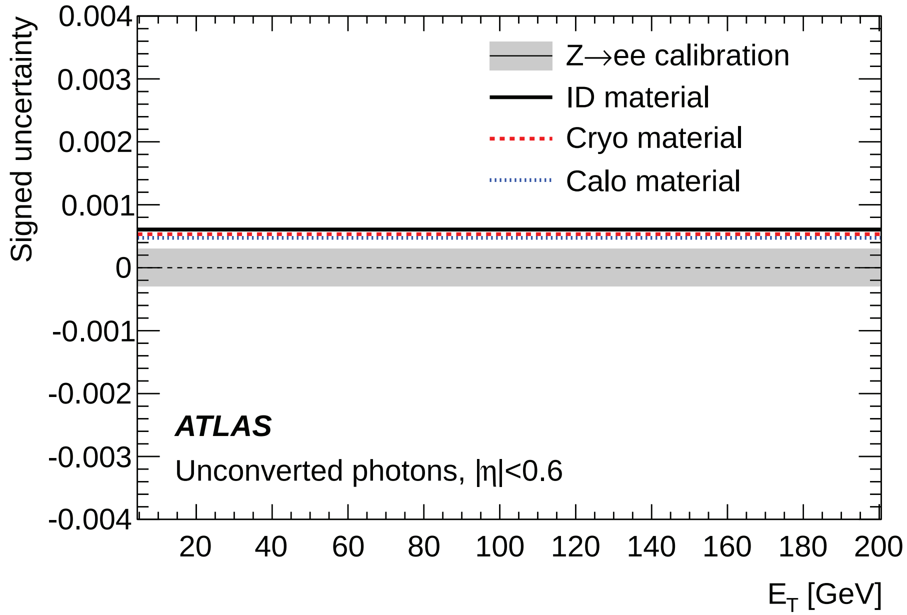

Electron and photon calibration in ATLAS (II)

ATLAS Collaboration, Eur. Phys. J. C74 (2014) 3071